 CMES, vol.34, no.2, pp.117-136, 2008

Assessment of Mixed Uniform Boundary Conditions for Predicting the Mechanical Behavior of Elastic and Inelastic Discontinuously Reinforced Composites

D. H. Pahr[1] **and H.J. Böhm**[1]

Abstract: The combination of heterogeneous volume elements and numerical analysis schemes such as the Finite Element method provides a powerful and well proven tool for studying the mechanical behavior of composite materials. Periodicity boundary conditions (PBC), homogeneous displacement boundary conditions (KUBC) and homogeneous traction boundary conditions (SUBC) have been widely used in such studies. Recently Pahr and Zysset (2008) proposed a special set of mixed uniform boundary conditions (MUBC) for evaluating the macroscopic elasticity tensor of human trabecular bone. These boundary conditions are not restricted to periodic phase geometries, but were found to give the same predictions as PBC for the effective elastic properties of periodic open cell microstructures of orthotropic symmetry. Accordingly, they have been referred to as "periodicity compatible MUBC" (PMUBC).
The present study uses periodic volume elements that contain randomly positioned spherical particles or randomly oriented short fibers at moderate volume fractions for assessing the applicability of PMUBC to modeling composite materials via volume elements that deviate from orthotropic symmetry. Macroscopic elasticity tensors are evaluated with PBC, PMUBC and KUBC for elastic contrasts in the range $2 \leq s_{\mathrm{r}} \leq 30$. For one configuration the isotropic contributions to the macroscopic elastic tensors obtained with PBC and PMUBC are extracted and compared. In addition, macroscopic elastic-plastic responses for different hardening behaviors are studied with PBC and PMUBC. Only small differences between the predictions obtained with PBC and PMUBC are found, validating the PMUBC for studying volume elements the overall behavior of which shows minor contributions of lower than orthotropic symmetry.

Keyword: Mixed Uniform Boundary Conditions, Periodicity Boundary Conditions, Finite Element Simulation, Composites

[1] Institute of Lightweight Design and Structural Biomechanics, Vienna University of Technology, A-1040 Vienna, Austria

1 Introduction

By applying numerical engineering methods such as the Finite Element Method (FEM) to the analysis of inhomogeneous volume elements (VEs) of various levels of geometrical complexity the mechanical behavior of inhomogeneous materials can be studied in considerable detail. Appropriate boundary conditions (BC) must be specified for the volume elements, standard choices being kinematically uniform (KUBC), statically uniform (SUBC), and periodicity (PBC) boundary conditions. SUBC lead to lower estimates and KUBC to upper estimates for the macroscopic stiffness, compare Nemat-Nasser and Hori (1993), and predictions based on PBC lie between the above, see e.g. Suquet (1987). Less well known are uniform displacement–traction (orthogonal mixed) boundary conditions (MUBC), which were proposed by Hazanov and Amieur (1995), Hazanov (1998) and Hazanov (1999). They give rise to predictions between those obtained with SUBC and KUBC as shown by the order relations of Ostoja-Starzewski (2006). The use of MUBC for obtaining apparent elastic moduli of inhomogeneous materials was reported, e.g., by Jiang, Ostoja-Starzewski, and Jasiuk (2002) and Ostoja-Starzewski (2006). Results generated with KUBC, SUBC and MUBC are apparent properties in the sense of Huet (1990) in that they pertain to samples of small size. The use of PBC, in contrast, implies studying periodic "model composites" and gives rise to effective material properties.

In elasticity a considerable range of mixed uniform boundary conditions are possible. A specific set of such boundary conditions was proposed by Pahr and Zysset (2008) for studying the macroscopic behavior of trabecular bone, a biological random cellular medium. It was found that for microscopically orthotropic materials (i.e., materials with phase arrangements of orthotropic symmetry) these MUBC give rise to exactly the same macroscopic elastic properties as do PBC. Accordingly, they are referred to as "periodicity compatible MUBC" (PMUBC).

Hazanov and Amieur (1995) as well as Hazanov (1998) showed that mixed uniform boundary conditions that fulfill the Hill condition, equation (2), must be orthogonal. In a strict sense, this limits their use to materials having at least orthotropic elastic symmetry at the macroscale and to volume elements that are aligned with the principal axes of orthotropy. The present work explores the applicability of PMUBC to periodic multi-inclusion VEs for modeling the mechanical behavior of discontinuously reinforced composite materials. Especially when they contain rather low numbers of randomly positioned particles or fibers, such volume elements tend to show low-symmetry contributions to their macroscopic responses and, accordingly, do not fully comply with the requirements stated above.

For assessing the validity of the resulting models, the two periodic volume elements

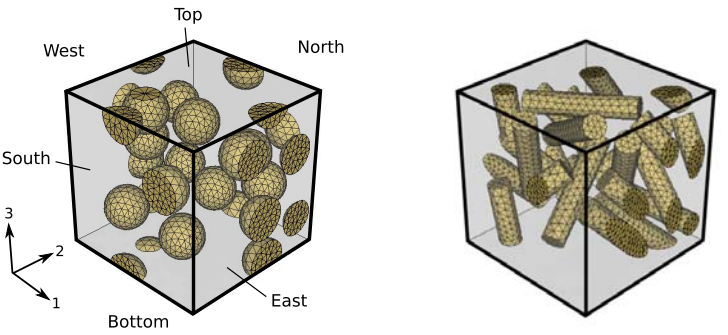

Figure 1: Periodic unit cells containing 15 spherical particles (right), and 15 randomly oriented cylindrical fibers (left) at a volume fraction of ξ=0.15 from Böhm, Han, and Eckschlager (2004). The six faces of the volume element are denoted as East, West, South, North, Bottom, and Top.

shown in Figure 1 are revisited. These "multi-inclusion unit cells" were used for studying the mechanical behavior of particle and short fiber reinforced composites of moderate reinforcement volume fraction by Böhm, Eckschlager, and Han (2002) as well as Böhm, Han, and Eckschlager (2004). In the present contribution predictions for the apparent and effective elasticity tensors and moduli evaluated for these VEs with KUBC, PMUBC and PBC are compared for elastic contrasts in the range $2 \leq s_{\mathrm{r}} \leq 30$. In addition, the macroscopic elastic-plastic responses under tensile loading obtained with PBC and PMUBC are assessed for different matrix hardening behaviors.

2 Methods

Numerical descriptors such as phase or volume averages of the microfields can be used for assessing the results obtained from three-dimensional multi-inclusion volume elements. The FEM code used in the present study, ABAQUS/Standard (Simulia, Providence, RI), provides an option for accessing the volume corresponding to a given integration point, so that the volume average of a function $f(x)$ can be approximated as

$$\langle f \rangle = \frac{1}{\Omega} \int_{\Omega} f(x)\, \mathrm{d}\Omega \approx \frac{1}{\Omega} \sum_{i=1}^{{}^{\mathrm{IP}}N} {}^{\mathrm{IP}}f_i \, {}^{\mathrm{IP}}\Omega_i \quad . \tag{1}$$

Here, ${}^{\mathrm{IP}}f_i$ and ${}^{\mathrm{IP}}\Omega_i$ are the function value and the integration point volume, respectively, associated with the i-th integration point, where the volume Ω contains ${}^{\mathrm{IP}}N$

integration points.

The macroscopic elasticity tensor of a volume element can be evaluated from the volume averaged stress and strain tensors obtained from six linearly independent load cases. From the components of this elasticity tensor, in turn, estimates for the macroscopic elastic moduli of the composite can be extracted.

2.1 Boundary Conditions

Table 1: The six linearly independent uniform strain load cases making up the periodicity compatible mixed boundary conditions (PMUBC) proposed by Pahr and Zysset (2008); East, West, North, South, Top, and Bottom denote the faces of the volume element, compare Figure 1 (left).

	East	West	North	South	Top	Bottom
Tensile 1	$u_1 = {}^0\varepsilon_{11}\frac{l_1}{2}$ $t_2 = t_3 = 0$	$u_1 = -{}^0\varepsilon_{11}\frac{l_1}{2}$ $t_2 = t_3 = 0$	$u_2 = 0$ $t_1 = t_3 = 0$	$u_2 = 0$ $t_1 = t_3 = 0$	$u_3 = 0$ $t_1 = t_2 = 0$	$u_3 = 0$ $t_1 = t_2 = 0$
Tensile 2	$u_1 = 0$ $t_2 = t_3 = 0$	$u_1 = 0$ $t_2 = t_3 = 0$	$u_2 = {}^0\varepsilon_{22}\frac{l_2}{2}$ $t_1 = t_3 = 0$	$u_2 = -{}^0\varepsilon_{22}\frac{l_2}{2}$ $t_1 = t_3 = 0$	$u_3 = 0$ $t_1 = t_2 = 0$	$u_3 = 0$ $t_1 = t_2 = 0$
Tensile 3	$u_1 = 0$ $t_2 = t_3 = 0$	$u_1 = 0$ $t_2 = t_3 = 0$	$u_2 = 0$ $t_1 = t_3 = 0$	$u_2 = 0$ $t_1 = t_3 = 0$	$u_3 = {}^0\varepsilon_{33}\frac{l_3}{2}$ $t_1 = t_2 = 0$	$u_3 = -{}^0\varepsilon_{33}\frac{l_3}{2}$ $t_1 = t_2 = 0$
Shear 12	$u_2 = {}^0\varepsilon_{21}\frac{l_1}{2}$ $u_3 = 0, t_1 = 0$	$u_2 = -{}^0\varepsilon_{21}\frac{l_1}{2}$ $u_3 = 0, t_1 = 0$	$u_1 = {}^0\varepsilon_{12}\frac{l_2}{2}$ $u_3 = 0, t_2 = 0$	$u_1 = -{}^0\varepsilon_{12}\frac{l_2}{2}$ $u_3 = 0, t_2 = 0$	$u_3 = 0$ $t_1 = t_2 = 0$	$u_3 = 0$ $t_1 = t_2 = 0$
Shear 13	$u_3 = {}^0\varepsilon_{31}\frac{l_1}{2}$ $u_2 = 0, t_1 = 0$	$u_3 = -{}^0\varepsilon_{31}\frac{l_1}{2}$ $u_2 = 0, t_1 = 0$	$u_2 = 0$ $t_1 = t_3 = 0$	$u_2 = 0$ $t_1 = t_3 = 0$	$u_1 = {}^0\varepsilon_{13}\frac{l_3}{2}$ $u_2 = 0, t_3 = 0$	$u_1 = -{}^0\varepsilon_{13}\frac{l_3}{2}$ $u_2 = 0, t_3 = 0$
Shear 23	$u_1 = 0$ $t_2 = t_3 = 0$	$u_1 = 0$ $t_2 = t_3 = 0$	$u_3 = {}^0\varepsilon_{32}\frac{l_2}{2}$ $u_1 = 0, t_2 = 0$	$u_3 = -{}^0\varepsilon_{32}\frac{l_2}{2}$ $u_1 = 0, t_2 = 0$	$u_2 = {}^0\varepsilon_{23}\frac{l_3}{2}$ $u_1 = 0, t_3 = 0$	$u_2 = -{}^0\varepsilon_{23}\frac{l_3}{2}$ $u_1 = 0, t_3 = 0$

Hill (1963) showed that the necessary and sufficient conditions for equivalence between the energetically and mechanically defined properties of elastic materials are contained in the so-called Hill condition

$$\langle \sigma : \varepsilon \rangle = \langle \sigma \rangle : \langle \varepsilon \rangle \quad . \tag{2}$$

This condition states that the volume average of the product of the microscopic stress and strain tensors, $\sigma(x)$ and $\varepsilon(x)$, equals the product of their volume averages, i.e., the macroscopic stresses and strains. Using the Gauss theorem the Hill condition can be transformed into the expression

$$\int_\Gamma \Big(t(x) - \langle \sigma \rangle n\Big) \cdot \Big(u(x) - \langle \varepsilon \rangle x\Big) \mathrm{d}\Gamma = 0 \quad , \tag{3}$$

compare Hazanov (1998). Here Γ is the boundary of a volume element and t, u, n, and x are the traction, displacement, surface normal, and position vectors,

respectively. For an infinite homogeneous body this condition is trivially satisfied, but for a finite heterogeneous volume it requires loading in specific ways on the boundary Γ. As was pointed out by Hazanov and Amieur (1995) as well as Ostoja-Starzewski (2006) this is the case for three types of uniform boundary conditions,

1. uniform displacement (Dirichlet, kinematic, KUBC) boundary conditions:

$$u(x) = {}^0\varepsilon\, x \qquad \forall x \in \Gamma \quad , \tag{4}$$

2. uniform traction (Neumann, static, SUBC) boundary conditions:

$$t(x) = {}^0\sigma\, n \qquad \forall x \in \Gamma \quad , \tag{5}$$

3. uniform displacement–traction (orthogonal mixed, MUBC) boundary conditions:

$$\Big(t(x) - {}^0\sigma\, n\Big) \cdot \Big(u(x) - {}^0\varepsilon\, x\Big) = 0 \qquad \forall x \in \Gamma\,, \tag{6}$$

where ${}^0\varepsilon$ and ${}^0\sigma$ denote constant tensors, prescribed *a priori* on the VE. In addition to the above cases, for periodic microstructures the Hill condition, equation (2), is fulfilled by periodicity boundary conditions (PBC), compare Suquet (1987), Anthoine (1995), Pahr (2003), as well as Pahr and Rammerstorfer (2006). Here, the boundary Γ must consist of pairs of parallel faces denoted as k^+ and k^-, for which the condition

$${}^{k^+}u(x) - {}^{k^-}u(x) = {}^0\varepsilon\, \Delta^k x \qquad \forall x \in {}^k\Gamma \tag{7}$$

holds, where $\Delta^k x$ is a constant distance vector between the two faces making up a pair.

MUBC that fulfill equation (6) can be obtained via different combinations of prescribed boundary vectors. Each such set of mixed BC yields a different apparent stiffness tensor. The special set of mixed boundary conditions referred to as PMUBC by Pahr and Zysset (2008) is summarized in Table 1, where l_1, l_2 and l_3 are the side lengths of the hexahedral VE in the 1-, 2- and 3-directions, respectively. The PMUBC can handle shear loading, which allows apparent elasticity tensors to be evaluated and thus extends earlier work using MUBC in elasticity, such as Hazanov (1998) as well as Jiang, Ostoja-Starzewski, and Jasiuk (2002). For periodic volume elements of orthotropic symmetry the PMUBC give the same predictions for the macroscopic elasticity tensor as do PBC. A related behavior of specific MUBC was reported by Jiang, Jasiuk, and Ostoja-Starzewski (2002) in the context of thermal conduction in two-dimensional composites.

Having been developed for the FE-based analysis of cellular materials, PMUBC are formulated to avoid prescribing nonzero boundary tractions. The boundary conditions compared in the present study, KUBC, PMUBC and PBC, can be directly applied to displacement based Finite Element models.

2.2 Finite Element Modelling

The periodic multi-inclusion unit cells employed for the present study contain 15 randomly positioned identical spheres or 15 randomly positioned and randomly oriented identical cylindrical fibers of aspect ratio a=5. The nominal reinforcement volume fraction of both VEs takes the moderate value of ξ=0.15.

The unit cells were each meshed with some 100000 10-node tetrahedral elements. Compatible meshes were enforced on pairs of opposite faces as required for specifying the periodicity BC. Note that the latter provision is necessary for PBC, but not for PMUBC, SUBC and KUBC.

The elastic behavior and the elastic-plastic responses of the unit cells under tensile loading were evaluated with ABAQUS/Standard, geometrically nonlinear analyses being employed for the inelastic models. An in-house code was used to define the multi-point constraints required for applying the periodicity boundary conditions. KUBC and PMUBC were implemented by specifying appropriate boundary displacements. SUBC are not considered in the present study.

The elastic-plastic material behavior of the matrix is described by J_2-plasticity with isotropic linear hardening, a linear elastic description is employed for the reinforcements, and a perfectly strong interface between reinforcements and matrix is specified. The material parameters used in the study are summarized in Table 2, where the Young's moduli E and the Poisson numbers ν of the two isotropic constituents are given. Different elastic contrasts, $s_R = E_I/E_M$, were obtained by varying the Young's modulus of the matrix, E_M. Simulations using a fixed initial yield stress $\sigma_{Y,M}$ combined with two different hardening moduli $E_{H,M}$ for the matrix as well as two elastic contrasts were employed for assessing the macroscopic elastic-plastic responses.

Three different tensile loading scenarios were investigated in the elastic-plastic regime: Macroscopic uniaxial strain conditions (positive displacements in the 1-direction plus zero displacements in the 2- and 3-directions), uniaxial stress conditions (positive displacements in the 1-direction plus unconstrained displacements in the 2- and 3-directions), as well as simple shear in the 12-plane with zero displacements in 3-direction. The second of these load cases cannot be generated with the PMUBC listed in Table 1, but appropriate mixed uniform boundary conditions can be obtained by replacing zero displacement components with zero traction compo-

Table 2: Material parameters used for the simulations. Five different elastic contrasts s_R and two different hardening moduli of the matrix material $E_{H,M}$ are investigated.

Property	Inclusion	Matrix (s_R=2/5/10/20/30)
Elastic (s_R=2/5/10/20/30)		
E (GPa)	400	200/80/40/20/13.3
ν	0.17	0.3
Plastic ("weak hardening"/"marked hardening")		
$\sigma_{Y,M}$ (MPa)	-	100
$E_{H,M}$ (MPa)	-	1/1900

nents in load case "Tensile 1" in Table 1. Results pertaining to the latter boundary conditions are denoted as "MUBC" in the following sections. The maximum macroscopic strains in the elastic-plastic analyses reached a value of 5%.

The number of reinforcements contained in the multi-inclusion unit cells shown in Figure 1 is insufficient for making them proper representative volume elements as discussed, e.g., by Hill (1963) or Stroeven, Askes, and Sluys (2004). The effective and apparent elastic properties obtained from these microgeometries deviate to some extent from the macroscopic isotropy associated with composites reinforced by spherical particles or randomly oriented fibers, compare Böhm, Han, and Eckschlager (2004). The latter behavior is actually desirable in the present context because it allows to assess the suitability of PMUBC for studying volume elements that show low-symmetry perturbations from the ideal macroscopic symmetry.

3 Results

3.1 Elastic Response

The "raw" elasticity tensors obtained from sets of six linearly independent load cases were orthotropized and, in the case of PMUBC, symmetrized, as discussed in section 4.1. Elastic moduli extracted from these tensors for the two volume elements are presented in Figures 2 and 3, where the relative differences of the macroscopic Young's moduli E (left), shear moduli G (center) and bulk moduli K (right) with respect to the pertinent PBC results are plotted as functions of the elastic contrast. Direction averages are shown for the Young's and shear moduli, and the minimum and maximum values due to the anisotropy of the volume elements are indicated by error bars. Proper representative volume elements for both

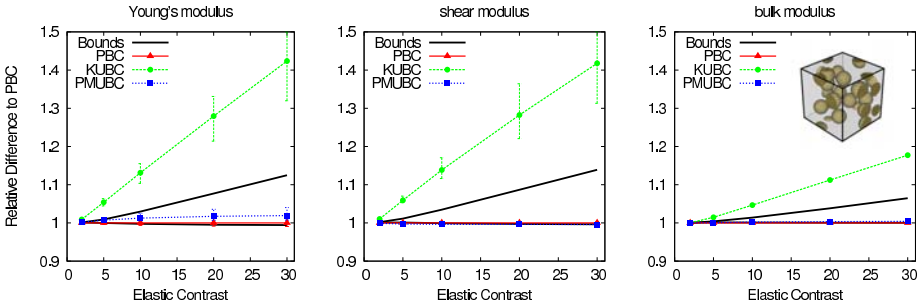

Figure 2: Elastic responses of composites reinforced by spheres of equal size: The relative differences between predictions obtained with PBC, PMUBC and KUBC for the Young's modulus (left), shear modulus (center), and bulk modulus (right) are shown as functions of the elastic contrast s_R. In addition the pertinent three-point bounds are given.

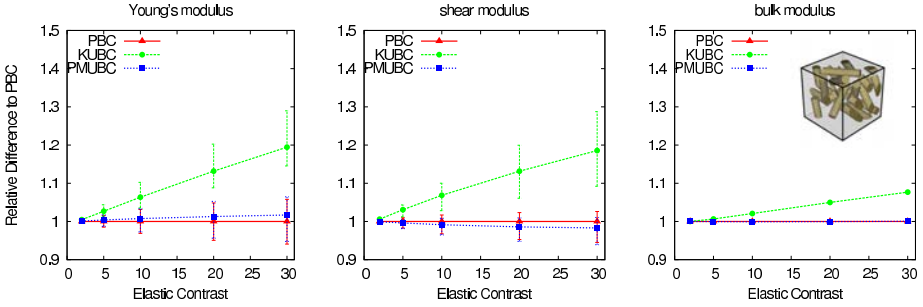

Figure 3: Elastic responses of composites reinforced by randomly oriented cylindrical fibers of aspect ratio $a = 5$: The relative differences between predictions obtained with PBC, PMUBC and KUBC for the Young's modulus (left), shear modulus (center), and bulk modulus (right) are shown as functions of the elastic contrast s_R.

types of composites must follow the bounds of Hashin and Shtrikman (1963) for the elastic behavior of macroscopically isotropic inhomogeneous materials. In addition, three point bounds as discussed, e.g., in Torquato (2002) are available for the sphere reinforced composite. These improved bounds were evaluated with statistical parameters for hard spheres of equal size proposed by Torquato, Lado, and Smith (1987) as well as Miller and Torquato (1990), are much tighter than bounds of Hashin and Shtrikman (1963) and are shown in Figure 2.

For the particle reinforced composite the predictions obtained with PBC and PMUBC are in excellent agreement for the shear and bulk moduli, with the estimates based on PMUBC tending to be slightly below the PBC values for G and slightly above them for K. The Young's moduli obtained with PMUBC show stronger anisotropy and their directional averages exceed those generated with PBC by up to 1.66%. At low elastic contrasts, where the bounds are very tight, the predictions obtained with PBC and PMUBC are slightly below the Hashin–Shtrikman and 3-point bounds, the relative difference being of order 10^{-3} or less. The apparent moduli obtained with the KUBC, while remaining within the Hashin–Shtrikman bounds, consistently exceed the three-point upper bounds, the difference to the PBC-based estimates being more than 40% for the macroscopic Young's and shear moduli.

Table 3: "Raw" macroscopic elasticity tensors $\mathbf{E}_{\mathrm{PBC,raw}}$ and $\mathbf{E}_{\mathrm{PMUBC,raw}}$ obtained from the short fiber reinforced volume element shown in Figure 1 (right) with a matrix Young's modulus of E_{M}=13.3 GPa.

$$\mathbf{E}_{\mathrm{PBC,raw}} = \begin{pmatrix} 23.87 & 9.58 & 10.16 & 0.01 & -0.25 & -0.22 \\ 9.58 & 25.12 & 10.10 & 0.22 & -0.16 & -0.26 \\ 10.16 & 10.10 & 26.94 & 0.63 & -1.01 & -0.08 \\ 0.01 & 0.22 & 0.63 & 7.90 & -0.11 & -0.20 \\ -0.25 & -0.16 & -1.01 & -0.11 & 7.94 & 0.09 \\ -0.22 & -0.26 & -0.08 & -0.20 & 0.09 & 7.27 \end{pmatrix}$$

$$\mathbf{E}_{\mathrm{PMUBC,raw}} = \begin{pmatrix} 23.88 & 9.54 & 10.00 & 0.04 & -0.17 & -0.16 \\ 9.54 & 25.79 & 9.97 & 0.10 & -0.18 & -0.21 \\ 10.00 & 9.96 & 26.78 & 0.38 & -0.73 & -0.03 \\ 0.00 & 0.05 & 0.20 & 7.77 & -0.02 & -0.23 \\ -0.14 & -0.22 & -0.89 & -0.06 & 7.70 & 0.10 \\ -0.14 & -0.25 & 0.04 & -0.25 & 0.06 & 7.22 \end{pmatrix}$$

The same trends are evident in the effective and apparent moduli evaluated for the composite reinforced by randomly oriented short fibers, see Figure 3. The direction dependence of the Young's and shear moduli, however, is more marked for this VE. With the exception of the bulk modulus for s_{R}=2 all numerical estimates fulfill the Hashin–Shtrikman bounds. Interestingly, the upper estimates obtained with the KUBC deviate from the PBC-based reference values to a lesser degree than is the case for the sphere reinforced composite.

Table 4: Phase averages of the stress components (in units of MPa) for the sphere reinforced unit cell shown in Figure 1 (left) at a macroscopic uniaxial strain of 0.1% in 1-direction predicted with PBC, PMUBC and the three-point estimates (TPE) of Torquato (1997). The Young's modulus of the matrix is set to E_M=13.3 GPa.

	PBC		PMUBC		TPE	
	Matrix	Particles	Matrix	Particles	Matrix	Particles
σ_{11}	20.79	36.86	20.78	38.25	20.78	37.45
σ_{22}	8.88	12.24	8.88	11.82	8.87	12.02
σ_{33}	8.88	12.06	8.88	11.83	8.87	12.02
σ_{12}	0.00	-0.21	0.02	0.09	0.0	0.0
σ_{13}	0.00	-0.38	-0.08	-0.74	0.0	0.0
σ_{23}	0.0	-0.09	-0.02	-0.09	0.0	0.0

Table 3 lists the "raw" macroscopic elasticity tensors obtained with PBC and PMUBC, $\mathbf{E}_{\mathrm{PBC,raw}}$ and $\mathbf{E}_{\mathrm{PMUBC,raw}}$, respectively, for the volume element containing randomly oriented short fibers shown in Figure 1 (right), which displays considerable macroscopic anisotropy. The two elasticity tensors are given in contracted Nye notation as 6×6 matrices (engineering shear strains being used in the strain quasi-vectors), pertain to a matrix Young's modulus of E_M=13.3 GPa, and are given in units of GPa.

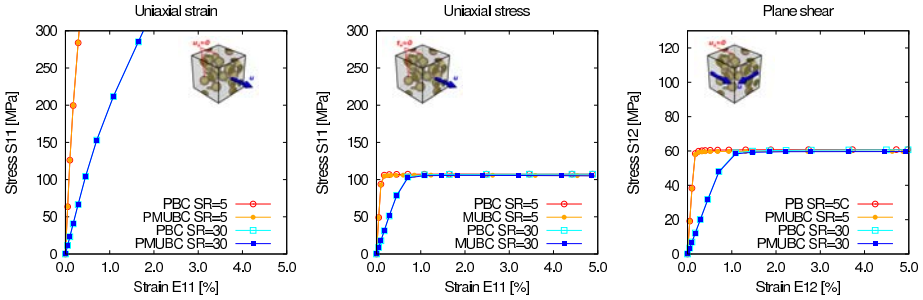

Figure 4: Elastic–plastic response of sphere reinforced composites with weak matrix hardening: Macroscopic stress–strain curves predicted with PBC and PMUBC for two different stiffness ratios and three tensile loading scenarios, uniaxial strain (left), uniaxial stress (center), and simple shear (right).

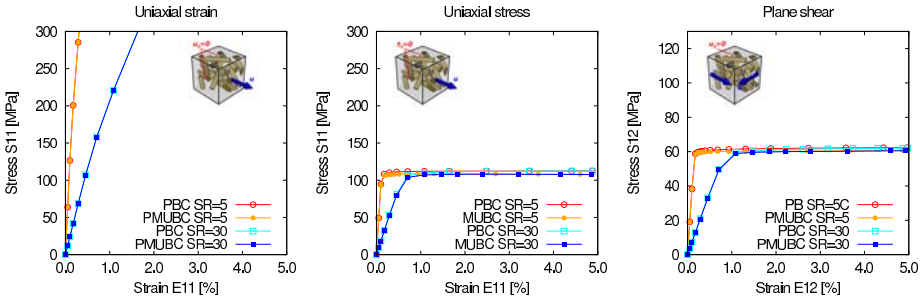

Figure 5: Elastic–plastic response of random short fiber reinforced composites with weak matrix hardening: Macroscopic stress–strain curves predicted with PBC and PMUBC for two different stiffness ratios and three tensile loading scenarios, uniaxial strain (left), uniaxial stress (center), and simple shear (right).

By applying equation (1) to integration points pertaining to either the reinforcements or the matrix, phase averages of the stress and strain tensors can be extracted from the FE results. Table 4 lists the phase averaged stress components evaluated with PBC and PMUBC for the sphere reinforced composite, Figure 1 (left), using a matrix Young's modulus of E_{M}=13.3 GPa and a macroscopic uniaxial tensile strain of 0.1%. In addition, predictions for the microfields obtained with the three-point estimates of Torquato (1997), marked as TPE, are given. As with the three-point bounds shown in Figures 2 and 3, the statistical parameters proposed by Torquato, Lado, and Smith (1987) as well as Miller and Torquato (1990) were used for evaluating the three-point estimates.

3.2 Elastic-Plastic Response

Figures 4 and 5 present the elastic-plastic responses to the three loading scenarios described in section 2.2 predicted for the two VEs when weak strain hardening was specified for the matrix. The axial and shear components of the macroscopic stresses are plotted versus the corresponding strain components, which were evaluated from volume averages of the nominal stresses and strains, respectively. The stresses and strains were obtained from ABAQUS at integration point level using equation (1). Two curves corresponding to elastic contrasts between inclusion and matrix of s_{r}=5 and s_{r}=30, respectively, are displayed in each plot. Excellent agreement between the predictions obtained with PBC and PMUBC/MUBC can be observed for both values of the elastic contrast considered. A close inspection shows some minor effects of the elastic contrast, the predictions obtained with the mixed uniform boundary conditions being minimally softer for the uniaxial stress

and shear load cases compared to the PBC results.

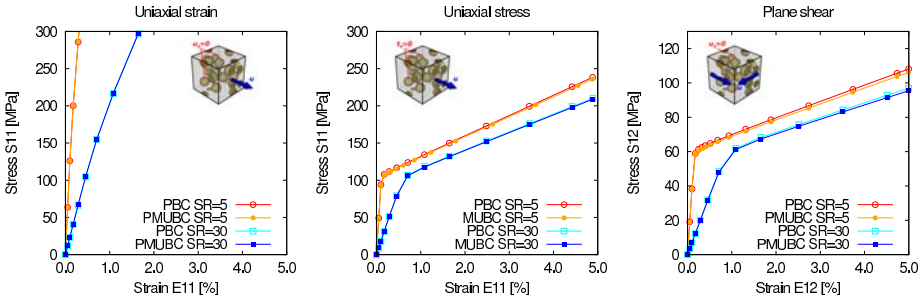

Figure 6: Elastic–plastic response of sphere reinforced composites with marked matrix hardening: Macroscopic stress–strain curves predicted with PBC and PMUBC for two different stiffness ratios and three tensile loading scenarios, uniaxial strain (left), uniaxial stress (center), and simple shear (right).

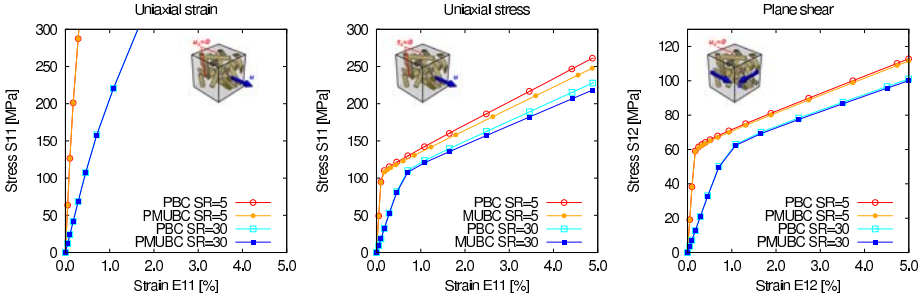

Figure 7: Elastic–plastic response of random short fiber reinforced composites with marked matrix hardening: Macroscopic stress–strain curves predicted with PBC and PMUBC for two different stiffness ratios and three tensile loading scenarios, uniaxial strain (left), uniaxial stress (center), and simple shear (right).

Analogous results obtained for a matrix material with marked strain hardening are displayed in Figures 6 and 7. The effect of matrix hardening is directly visible in the predicted macroscopic stress–strain curves. For the composite reinforced by randomly oriented short fibers subjected to uniaxial tensile stress the differences between the predictions obtained with the two sets of boundary conditions are more pronounced than for the other situations considered, the mixed uniform BC leading to slightly lower macroscopic hardening.

4 Discussion

For phase arrangements that show mirror symmetry with respect to three mutually normal planes the PMUBC listed in Table 1 are directly related to periodic solutions. Accordingly, they provide effective elasticities for orthotropic composites, whereas apparent elasticity tensors are returned for microgeometries of lower symmetries. PBC, which are based on translatory symmetry, are not restricted in terms of the macroscopic symmetries of VEs and, accordingly, are well suited to providing reference solutions against which predictions obtained with PMUBC can be checked. Multi-inclusion unit cells employing a low number of reinforcements approach macroscopic isotropy but display low-symmetry contributions to their overall response. Accordingly, they provide suitable scenarios for assessing the applicability of PMUBC to VEs that are not perfectly orthotropic.

4.1 Elastic Response

Table 5: Orthotropized and, where applicable, symmetrized macroscopic elasticity tensors $\mathbf{E}_{\mathrm{PBC,ortho}}$ and $\mathbf{E}_{\mathrm{PMUBC,ortho}}$ obtained from the "raw" elasticity tensors listed in table 3 for the short fiber reinforced volume element shown in Figure 1 (right) with a matrix Young's modulus of E_{M}=13.3 GPa.

$$\mathbf{E}_{\mathrm{PBC,ortho}} = \begin{pmatrix} 23.87 & 9.58 & 10.16 & 0 & 0 & 0 \\ 9.58 & 25.12 & 10.10 & 0 & 0 & 0 \\ 10.16 & 10.10 & 26.94 & 0 & 0 & 0 \\ 0 & 0 & 0 & 7.90 & 0 & 0 \\ 0 & 0 & 0 & 0 & 7.94 & 0 \\ 0 & 0 & 0 & 0 & 0 & 7.27 \end{pmatrix}$$

$$\mathbf{E}_{\mathrm{PMUBC,ortho}} = \begin{pmatrix} 23.88 & 9.54 & 10.00 & 0 & 0 & 0 \\ 9.54 & 25.79 & 9.97 & 0 & 0 & 0 \\ 10.00 & 9.97 & 26.78 & 0 & 0 & 0 \\ 0 & 0 & 0 & 7.77 & 0 & 0 \\ 0 & 0 & 0 & 0 & 7.70 & 0 \\ 0 & 0 & 0 & 0 & 0 & 7.22 \end{pmatrix}$$

This section concentrates on the macroscopic elasticity tensors obtained with PBC and PMUBC from the volume element displayed in Figure 1 (right), which contains

15 randomly oriented short fibers and shows noticeable macroscopic anisotropy. The pertinent "raw" elasticity tensors, $\mathbf{E}_{\mathrm{PBC,raw}}$ and $\mathbf{E}_{\mathrm{PMUBC,raw}}$, see Table 5, may be viewed as consisting of two parts, viz., tensor components that are nonzero in an orthotropic elasticity tensor in principal orientation (in Nye notation, the matrix elements in the upper left 3×3 submatrix and the lower left diagonal) and "anisotropic coupling terms" (all other tensor components). Both sets of components show some anisotropy and direction dependence in each tensor, the anisotropic coupling terms being at least an order of magnitude smaller than the orthotropic ones for the example considered. The elasticity tensor obtained with PBC is perfectly symmetric, whereas the one evaluated using PMUBC shows some asymmetry, which is due to applying these boundary conditions to a VE of sub-orthotropic macroscopic symmetry. This asymmetry tends to grow with decreasing macroscopic symmetry of the volume element and with increasing elastic contrast of the constituents. The asymmetry of the "raw" elasticity tensors can be removed by symmetrization to obtain a proper elasticity tensor. Both $\mathbf{E}_{\mathrm{PBC,raw}}$ and $\mathbf{E}_{\mathrm{PMUBC,raw}}$ were "orthotropized" by setting the anisotropic coupling terms to zero. When this procedure is applied to the "raw" tensors listed in table 3, the tensors $\mathbf{E}_{\mathrm{PBC,ortho}}$ and $\mathbf{E}_{\mathrm{PMUBC,ortho}}$ presented in Table 5 are obtained. Tensors of this type were used in generating Figures 2 and 3.

Further improvements of the estimates for the macroscopic elasticity tensors can be achieved by invoking the known overall elastic isotropy of the composites to be modeled. For the two volume elements considered here this implies finding the isotropic elasticity tensors that are closest to $\mathbf{E}_{\mathrm{PBC,ortho}}$ and $\mathbf{E}_{\mathrm{PMUBC,ortho}}$, respectively. Such isotropic macroscopic elasticity tensors, $\mathbf{E}_{\mathrm{PBC,iso}}$ and $\mathbf{E}_{\mathrm{PMUBC,iso}}$, can be obtained in the form of the isotropic term of a generalized spherical harmonics expansion of the orthotropic elongation and bulk modulus orientation distribution functions, using the expressions developed by He and Curnier (1997). Table 6 lists the isotropic elasticity tensors obtained this way from $\mathbf{E}_{\mathrm{PBC,ortho}}$ and $\mathbf{E}_{\mathrm{PMUBC,ortho}}$.

From the above isotropic elasticity tensors estimates of $E_{\mathrm{PBC,iso}} = 19.69$ GPa and $E_{\mathrm{PMUBC,iso}} = 19.90$ GPa for the macroscopic Young's modulus, $G_{\mathrm{PBC,iso}} = 7.68$ GPa and $G_{\mathrm{PMUBC,iso}} = 7.77$ GPa for the macroscopic shear modulus, as well as $K_{\mathrm{PBC,iso}} = 15.05$ GPa and $K_{\mathrm{PMUBC,iso}} = 15.12$ GPa for the macroscopic bulk modulus were evaluated. Despite the anisotropy of the underlying volume element good agreement is evident between results obtained with PBC and PMUBC, the relative errors in terms of the moduli being less than 1.2%. The estimates for the macroscopic moduli fall within the Hashin–Shtrikman bounds and are close to the lower bounds.

Phase averaged stress components evaluated via equation (1) from macroscopic uniaxial tensile strain analysis using PBC and PMUBC, respectively, are listed

Table 6: Isotropic macroscopic elasticity tensors $\mathbf{E}_{\mathrm{PBC,iso}}$ and $\mathbf{E}_{\mathrm{PMUBC,iso}}$ obtained from the orthotropized elasticity tensors listed in table 5 for the short fiber reinforced volume element shown in Figure 1 (right) with a matrix Young's modulus of E_{M}=13.3 GPa.

$$\mathbf{E}_{\mathrm{PBC,iso}} = \begin{pmatrix} 25.29 & 9.93 & 9.93 & 0 & 0 & 0 \\ 9.93 & 25.29 & 9.93 & 0 & 0 & 0 \\ 9.93 & 9.93 & 25.29 & 0 & 0 & 0 \\ 0 & 0 & 0 & 7.68 & 0 & 0 \\ 0 & 0 & 0 & 0 & 7.68 & 0 \\ 0 & 0 & 0 & 0 & 0 & 7.68 \end{pmatrix}$$

$$\mathbf{E}_{\mathrm{PMUBC,iso}} = \begin{pmatrix} 25.48 & 9.94 & 9.94 & 0 & 0 & 0 \\ 9.94 & 25.48 & 9.94 & 0 & 0 & 0 \\ 9.94 & 9.94 & 25.48 & 0 & 0 & 0 \\ 0 & 0 & 0 & 7.77 & 0 & 0 \\ 0 & 0 & 0 & 0 & 7.77 & 0 \\ 0 & 0 & 0 & 0 & 0 & 7.77 \end{pmatrix}$$

in Table 4. These phase averages correspond to the "raw" elasticity tensors and show clear evidence of the anisotropy of the underlying unit cell. Even though the macroscopic load case is uniaxial strain, the shear components of the phase averaged stresses and, by implication, of the macroscopic stresses obtained with both PBC and PMUBC do not vanish, i.e., there is coupling between the normal and shear terms. In contrast, the stress tensor evaluated with the three-point estimates, which pertain to perfectly isotropic behavior, shows no such effects. The agreement between the phase averaged stresses evaluated with PBC and PMBUC is good, especially for the matrix averages of the normal stress components.

Taken together, the above results indicate that PMUBC are a valid choice for modeling the elastic behavior of composites with statistically isotropic macroscopic behavior when periodic volume elements containing a sufficiently high number of reinforcements are used to approximate macroscopic isotropy. In addition, PMUBC are well suited for application to "simply periodic" unit cells describing, e.g., cubic arrangements of spheres or hexagonal arrays of fibers, which by design have higher than orthotropic macroscopic symmetry. Some care is required, however, when PMUBC are applied to VEs the macroscopic behavior of which shows con-

siderable contributions with sub-orthotropic symmetries, such as volume elements containing a very small number of randomly positioned reinforcements. For the VEs considered in the present study, PMUBC always gave rise to estimates that are markedly closer to the solutions for periodic composites than are results obtained with kinematically uniform boundary conditions.

4.2 Elastic-Plastic Response

The results of the simulations of the elastic-plastic response of the volume elements under loading conditions pertinent to materials characterization presented in Figures 4 to 7 show very good agreement between results obtained with PBC and PMUBC. The only case where differences are non-trivial is that of randomly oriented fibers under macroscopic uniaxial tensile stress and using strong matrix hardening. However, whereas in the elastic regime the superposition principle allows any macroscopic stress or strain state to be modelled on the basis of the six independent load cases defining the PMUBC as listed in Table 1, path dependence in the elastic-plastic regime acts to markedly restrict the states attainable by this set of boundary conditions. In general, PBC are much more flexible in modeling the elastic-plastic and other non-linear behaviors of composites compared to PMUBC and the latter are not applicable to general multi-scale analysis.

4.3 Computational Issues

Another issue of interest are the requirements in terms of computation time and memory usage posed by FE simulations employing PBC and PMUBC. As is evident from their definition in Table 1, PMUBC imply displacement controlled analysis. Periodicity boundary conditions, in contrast, can be combined with both displacement and load control, the same unique estimate for the overall elastic tensor being obtained. Load controlled procedures typically are computationally more efficient for obtaining the elasticity tensor in displacement-based FE procedures, because evaluating and inverting the global stiffness matrix once is sufficient for analyzing the required six linearly independent load cases. Displacement control, in contrast, requires carrying out the above operations for each of the six load cases. Consequently, for periodic VEs the combination of load controlled analysis with PBC typically poses the lowest requirements in terms of CPU time. If only displacement controlled analysis is considered a different picture emerges. In such situations PMUBC are markedly more efficient than PBC because the multi-point constraints required for the latter set of boundary conditions substantially increase the bandwidth of the system equations. Figure 8 shows normalized data on CPU time and memory usage obtained for the two multi-inclusion unit cells shown in Figure 1 using a work station with 4 Xeon 5160 processors and 64 GByte of mem-

ory, on which the analyses ran in-core. Note that PMUBC are less memory intensive than PBC, the multi-point constraints required for implementing the latter degrading the band structure of the system matrix. This may translate into advantages for PMUBC when very large models are studied or when memory resources are very limited.

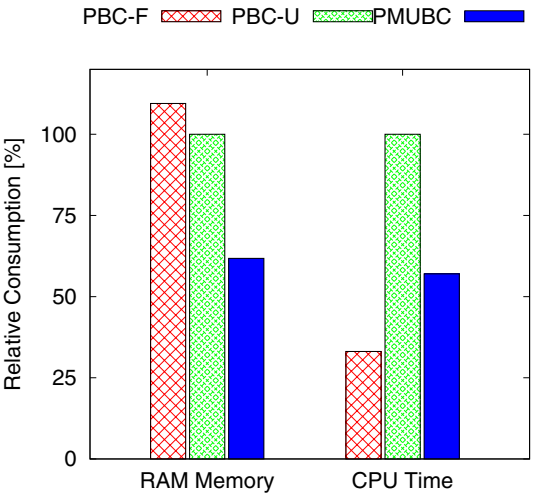

Figure 8: Comparison of memory usage (left) and required CPU time (right) pertaining to the multi-inclusion unit cells shown in Figure 1 evaluated with PBC for displacement controlled (PBC-U) and load controlled (PBC-F) analyses as well as PMUBC.

PMUBC enjoy a practical advantage over PBC with respect to preprocessing because the former do not require compatible meshes on opposite faces of volume elements, which can considerably simplify meshing. In addition, the prescribed displacements are constant and the prescribed tractions are zero over any given face, making PMUBC easier to handle with general-purpose FE preprocessors compared to KUBC and, especially, SUBC.

The scope of the present study is restricted to periodic volume elements for which predictions based on PMUBC can be compared against reference results obtained with PBC. A major strength of PMUBC, however, is that they do not require periodic phase arrangements. The main conclusions of the above discussion, viz. that — provided the the behavior of the volume element shows only small deviations from macroscopic orthotropy — PMUBC give excellent predictions for the apparent elasticity tensors and for the elastic-plastic stress–strain responses along

attainable load paths, can be expected to hold for non-periodic microgeometries, too. Such behavior was reported by Pahr and Zysset (2008).

5 Summary

A special set of mixed uniform boundary conditions proposed by Pahr and Zysset (2008) were applied to periodic multi-inclusion unit cells used in previous work for modelling the macroscopic elastic-plastic behavior of MMCs reinforced by particles or randomly oriented fibers at moderate volume fractions. A considerable range of elastic contrasts of the constituents as well as weak and strong strain hardening of the matrix were studied. PMUBC were found to give valid results for all cases considered which, on the one hand, allows the conclusion that they can be a useful alternative to periodicity boundary conditions when periodic volume elements are used to study the mechanical behavior of matrix–inclusion composites. On the other hand, PMUBC are not limited to periodic phase arrangements and, accordingly, provide an attractive option for studying non-periodic microgeometries.

Acknowledgement: Discussions with P. Zysset are gratefully acknowledged.

References

Anthoine, A. (1995): Derivation of the in-plane elastic characteristics of masonry through homogenization theory. *Int. J. Sol. Struct.*, vol. 32, pp. 137–163.

Böhm, H.; Eckschlager, A.; Han, W. (2002): Multi-inclusion unit cell models for metal matrix composites with randomly oriented discontinuous reinforcements. *Comput. Mater. Sci.*, vol. 25, pp. 42–53.

Böhm, H.; Han, W.; Eckschlager, A. (2004): Multi-inclusion unit cell studies of reinforcement stresses and particle failure in discontinuously reinforced ductile matrix composites. *CMES: Computer Modeling in Engineering & Sciences* , vol. 5, pp. 5–20.

Hashin, Z.; Shtrikman, S. (1963): A variational approach to the theory of the elastic behavior of multiphase materials. *J. Mech. Phys. Sol.*, vol. 11, pp. 127–140.

Hazanov, S. (1998): Hill condition and overall properties of composites. *Arch. Appl. Mech.*, vol. 68, pp. 385–394.

Hazanov, S. (1999): On apparent properties of nonlinear heterogeneous bodies smaller than the representative volume. *Acta Mech.*, vol. 134, pp. 123–134.

Hazanov, S.; Amieur, M. (1995): On overall properties of elastic bodies smaller than the representative volume. *Int. J. Engng. Sci.*, vol. 33, pp. 1289–1301.

He, Q.; Curnier, A. (1997): A more fundamental approach to damaged elastic stress–strain relations. *Int. J. Sol. Struct.*, vol. 32, pp. 1433–1457.

Hill, R. (1963): Elastic properties of reinforced solids: Some theoretical principles. *J. Mech. Phys. Sol.*, vol. 11, pp. 357–372.

Huet, C. (1990): Application of variational concepts to size effects in elastic heterogeneous bodies. *J. Mech. Phys. Sol.*, vol. 38, pp. 813–841.

Jiang, M.; Jasiuk, I.; Ostoja-Starzewski, M. (2002): Apparent thermal conductivity of periodic two-dimensional composites. *Comput. Mater. Sci.*, vol. 25, pp. 329–338.

Jiang, M.; Ostoja-Starzewski, M.; Jasiuk, I. (2002): Apparent elastic and elastoplastic behavior of periodic composites. *Int. J. Sol. Struct.*, vol. 39, pp. 199–212.

Miller, C.; Torquato, S. (1990): Effective conductivity of hard sphere suspensions. *J. Appl. Phys.*, vol. 68, pp. 5486–5493.

Nemat-Nasser, S.; Hori, M. (1993): *Micromechanics: Overall Properties of Heterogeneous Solids*. North–Holland, Amsterdam, The Netherlands.

Ostoja-Starzewski, M. (2006): Material spatial randomness: From statistical to representative volume element. *Probab. Engng. Mech.*, vol. 21, pp. 112–131.

Pahr, D. (2003): *Experimental and Numerical Investigations of Perforated FRP-Laminates*. Fortschritt-Berichte, Reihe **18**, Nr. 284. VDI–Verlag, Düsseldorf, FRG.

Pahr, D.; Zysset, P. (2008): Influence of boundary conditions on computed apparent elastic properties of cancellous bone. *Biomech. Model. Mechanobiol.* in print, doi: 10.1007/s10237-007-0109-7.

Pahr, D. H.; Rammerstorfer, F. G. (2006): Buckling of honeycomb sandwiches: Periodic finite element considerations. *CMES: Computer Modeling in Engineering & Science*, vol. 12, pp. 229–242.

Stroeven, M.; Askes, H.; Sluys, L. (2004): Numerical determination of representative volumes for granular materials. *Comput. Meth. Appl. Mech. Engng.*, vol. 193, pp. 3221–3238.

Suquet, P. (1987): Elements of homogenization for inelastic solid mechanics. In Sanchez-Palencia, E.; Zaoui, A.(Eds): *Homogenization Techniques in Composite Media*. Springer–Verlag, Berlin.

Torquato, S. (1997): Effective stiffness tensor of composite media: I. exact series expansions. *J. Mech. Phys. Sol.*, vol. 45, pp. 1421–1448.

Torquato, S. (2002): *Random Heterogeneous Media*. Springer–Verlag. New York, NY.

Torquato, S.; Lado, F.; Smith, P. (1987): Bulk properties of two-phase disordered media. iv. mechanical properties of suspensions of penetrable spheres at nondilute concentrations. *J. Chem. Phys.*, vol. 86, pp. 6388–6392.